

RSC Advances



This is an *Accepted Manuscript*, which has been through the Royal Society of Chemistry peer review process and has been accepted for publication.

Accepted Manuscripts are published online shortly after acceptance, before technical editing, formatting and proof reading. Using this free service, authors can make their results available to the community, in citable form, before we publish the edited article. This *Accepted Manuscript* will be replaced by the edited, formatted and paginated article as soon as this is available.

You can find more information about *Accepted Manuscripts* in the [Information for Authors](#).

Please note that technical editing may introduce minor changes to the text and/or graphics, which may alter content. The journal's standard [Terms & Conditions](#) and the [Ethical guidelines](#) still apply. In no event shall the Royal Society of Chemistry be held responsible for any errors or omissions in this *Accepted Manuscript* or any consequences arising from the use of any information it contains.

ARTICLE

Graphene oxide supported MnO₂ Nanorods: An efficient heterogeneous catalyst for oxidation of aromatic amines to azo-compounds

Cite this: DOI: 10.1039/x0xx00000x

Shweta Kumari, Amiya Shekhar, and Devendra D. Pathak*

Received 00th January 2012,
Accepted 00th January 2012

DOI: 10.1039/x0xx00000x

www.rsc.org/

Graphene oxide supported MnO₂ nanorods (GOnc), a composite material, has been synthesized and characterized by XRD, FE-SEM, EDX, BET surface area measurement, FTIR and Raman Spectroscopy. The composite material (GOnc) was found to be a highly efficient, reusable and cost effective heterogeneous catalyst for the one-pot, selective synthesis of azo-compounds from aromatic amines under N₂ atmosphere. After completion of the reaction, the catalyst is readily recovered by filtration and can be reused at least three times without significant loss in activity.

Introduction

Graphene oxide (GO) is one of the most important derivatives of graphene.¹ GO has attracted tremendous attention of scientists due to its remarkable physical, chemical, and electrical properties.² In recent years, GO has been used as an ideal support for a number of metals, metal oxides, inorganic complexes, and organic compounds due to its high specific surface area.³ Composite materials of GO have found applications in super capacitors, lithium ion batteries, semiconductor devices, catalysis, and biosensors.⁴ GO supported metal oxide nanoparticles is an emerging class of heterogeneous catalysts for facilitating synthetically useful organic transformations.⁵ Metal nanoparticles (NPs) are implicated in many industrial reactions, predominantly as heterogeneous catalysts.⁶ MnO₂ nanoparticles have been used as heterogeneous catalyst for oxidation reactions owing to its large number of active sites.⁷

Azo-compounds are widely used as organic dyes, indicators, food additives, drugs, radical reaction initiators, therapeutic agents, photochemical molecular switches, molecular shuttles, storage media, liquid crystals, nanotubes and in the manufacture of protective eye glasses and filters.^{8,9} The synthesis of azo-compounds have been reported in literature by several methods such as azo coupling reaction, Mills reaction, Wallach reactions, reduction of azoxybenzenes, oxidation of amines, dehydrogenation of arylhydrazines, reaction of quinone acetals with arylhydrazines, opening of benzotriazoles, thermolysis of azides, dimerization of diazonium salts, metal catalyzed coupling of arylhydrazines, and triazene rearrangements.¹⁰ However, among these methods, oxidation of amines is one of the easiest one-step routes for the synthesis of azo-compounds. A perusal of the literature reveals that oxidation of amines have been accomplished by several catalysts, such as silver nanoparticles, gold nanoparticles immobilized on TiO₂, nickel peroxide, NaBO₃, Pb(OAc)₄, MnO₂, BaMnO₄, Ce(OH)₃O₂H, RuCl₃/H₂O₂, Ag₂CO₃, AgMnO₄,

galvinoxyl/K₃Fe(CN)₆, KO₂, t-BuOCl, t-BuOI, Cu(I)-diaziridinone, and palladium and platinum nanowires.¹¹ However, many of these reported synthetic protocols suffer from one or more disadvantages, such as prolong reaction time, moderate yields, use of expensive catalyst, and formation of large amount of by-products. Depending upon the nature of the catalyst and the reaction conditions, oxidation of amines have been reported to yield azo-, azoxy-, nitro- and nitroso-compounds.¹² Therefore, the rational design of selective catalysts which could minimize the formation of by-products and exclusively yield the desired azo-compounds is one of the challenging areas of research.¹³

Herein, we report the synthesis of a composite material, i.e. graphene oxide supported MnO₂ nanorods (GOnc) and demonstrates its application as a selective, inexpensive, reusable and efficient heterogeneous catalyst for the synthesis of azo-compounds in one-step from amines in high yields.

Experimental

Preparation of MnO₂ nanorods

The MnO₂ nanorods were prepared by slight modification of reported method.¹⁴ 5 mM (0.1223 mL) hydrochloric acid (HCl) was mixed with 1.0 mM (0.158034 g) potassium permanganate (KMnO₄) solution and magnetically stirred for 30 min. The solution was transferred into a Teflon-lined stainless steel autoclave and hydrothermally treated at 120 °C for 10 h. The resultant black precipitate was collected by centrifugation.

Preparation of Graphene oxide supported MnO₂ nanorods (GOnc)

Initially, GO was prepared from graphite powder by using the modified Hummer's method.¹⁵ GOnc was prepared by modification of literature procedure.¹⁶ In brief, preparation of 1:1 ratio of

MnO₂/GO, 0.050 g of GO was dissolved in 30 mL de-ionized water followed by the addition of 1.0 mM (0.158034 g) of KMnO₄. 5 mM (0.1223 mL) HCl was added to the above mixture and the resultant mixture was magnetically stirred for 30 min at room temperature. The solution was transferred into a Teflon-lined stainless steel autoclave and hydrothermally treated at 120°C for 10 h. The resultant precipitate was collected by centrifugation, washed several times with deionised water and finally dried in vacuum.

Characterizations

The synthesised GO and GOnC were characterized by Powder X-ray diffraction (PANalytical Empyrean). Morphology of the GO, MnO₂ nanorods and GOnC were observed by Field Emission-Scanning Electron Microscopy (FE-SEM, Supra 55 Carl Zeiss, Germany). The composition of the GO and GOnC were determined by Energy-dispersive X-ray spectroscopy (EDX) analysis on a (Electron Probe Microscope Oxford X-MAX[®]). Raman spectra of GO, GOnC were recorded on a (High Resolution Raman Microspectrometer). Surface area of the GOnC was measured by a Brunauer-Emmett-Teller (BET) surface area analyzer (Quantumchrome Instrument 3200 Nova E). The FT-IR spectra were recorded on a (Perkin- Elmer RXI FT-IR Spectrometer) in KBr pellet. The ¹H NMR spectra of organic products were recorded in CDCl₃ on a (Bruker's advance III 400 MHz FT-NMR) at room temperature.

Synthesis and Characterization of azo-compounds

To a stirred solution of amine (1 mmol) in 1,2-dichloroethane (5 mL), GOnC (5 wt %) was added to the reaction mixture under reflux for specific time (4-18 hr) under nitrogen atmosphere. The progress of the reaction was monitored by TLC at regular intervals. After completion, the reaction mixture was cooled to room temperature and the GOnC catalyst removed by filtration. The GOnC was further washed with acetone (2x5 mL) and then dried under vacuum for reuse. Then reaction mixture was treated with water and the aqueous phase extracted with ethyl acetate (2x10 mL). The combined organic layers were treated with saturated brine solution and dried over anhydrous sodium sulphate. The removal of solvent yielded a crude solid which was purified by flash chromatography over Silica gel to afforded the desired azo-compounds.

The Physical and spectral data of synthesized azo compounds are given below:

Azobenzene (**2a**) orange solid; mp 65-66 °C (lit.)¹¹ 64-66 °C; IR: 3001, 1585, 1481, 1452, 1070, 782, 680 cm⁻¹; ¹H NMR (400 MHz, CDCl₃) δ 7.19-7.42 (m, 6H), 7.89-7.90 (m, 4H).

4,4'- Dimethylazobenzene (**2b**) light orange solid; mp 145-146 °C (lit.)¹¹ 142-146 °C; IR (KBr): 3424, 2905, 1585, 1485, 1139, 813, 700 cm⁻¹; ¹H NMR (400 MHz, CDCl₃) δ 2.43 (s, 6H), 7.25-7.31 (d, *J*=7.8 Hz 4H), 7.75-7.89 (d, *J*=7.8 Hz 4H).

4,4'-Dimethoxyazobenzene (**2c**) brown solid; mp 149-151 °C (lit.)¹¹ 150-152 °C; IR (KBr): 3085, 2833, 1589, 1569, 1497, 1240, 839 cm⁻¹; ¹H NMR (400 MHz, CDCl₃) δ 3.72 (s, 6H), 7.00-7.13 (d, *J*=8.1 Hz 4H), 7.69-7.72 (d, *J*=8.1 Hz 4H).

4,4'-Dibromoazobenzene (**2d**) reddish orange powder; mp 203-204 °C (lit.)¹¹ 200-201 °C ; IR (KBr): 3449, 1569, 1465, 1398, 1061, 849

cm⁻¹; ¹H NMR (400 MHz, CDCl₃) δ 7.61-7.65 (d, *J*=8.5 Hz 4H), 7.72-7.79 (d, *J*=8.5 Hz 4H).

4,4'-Dichloroazobenzene (**2e**) orange solid; mp 184-185 °C (lit.)¹¹ 182-185 °C; IR (KBr): 3438, 1559, 1482, 1092, 999, 841 cm⁻¹; ¹H NMR (400 MHz, CDCl₃) δ 7.51-7.56 (d, *J*=8.1 Hz 4H), 7.89-7.92 (d, *J*=8.1 Hz 4H).

2,2'-Dinitroazobenzene (**2f**) red solid; IR (KBr): 3046, 1550, 1542, 1230, 849 cm⁻¹; ¹H NMR (400 MHz, CDCl₃) δ 7.72-7.84 (m, 4H), 8.19-8.39 (m, 4H).

2,2'-Dimethylazobenzene (**2g**) red solid; mp 53-54 °C (lit.)¹¹ 51-55°C; IR (KBr): 3450, 2919, 1461, 1110, 1039, 766, 710 cm⁻¹; ¹H NMR (400 MHz, CDCl₃) δ 2.69 (s, 6H), 7.20-7.26 (m, 2H), 7.27-7.31 (m, 4H), 7.61-7.64 (m, 2H).

2,2'-Dichloroazobenzene (**2h**) orange solid; mp 137-138 °C (lit.)¹¹ 135-136°C; IR (KBr): 3051, 1582, 1511, 1452, 1241, 1072, 1043, 949, 756 cm⁻¹; ¹H NMR (400 MHz, CDCl₃) δ 7.31-7.40 (m, 4H), 7.58-7.60 (m, 4H).

2,2'-Difluoroazobenzene (**2i**) orange solid; mp 99-101 °C (lit.)¹¹ 100-101°C; IR (KBr): 1580, 1481, 1253, 1110, 849 cm⁻¹; ¹H NMR (400 MHz, CDCl₃) δ 7.19-7.26 (m, 4H), 7.40-7.26 (m, 2H), 7.79-7.82 (m, 2H).

3,3'-Dimethylazobenzene (**2j**) dark orange solid; mp 50-51 °C (lit.)¹¹ 50-51°C; IR (KBr): 2920, 1609, 1457, 1251, 791, 694 cm⁻¹; ¹H NMR (400 MHz, CDCl₃) δ 2.41 (s, 6H), 7.26-7.30 (m, 2H), 7.40-7.45 (m, 2H), 7.69 (m, 4H).

Results and discussion

The chemical and structural features of GO and GOnC were elucidated by FE-SEM, EDX, Raman, XRD, and FTIR, analyses. The FE-SEM images (Fig.1) depicts the surface morphology of MnO₂ nanorods, GO, and GOnC, respectively. From (Fig. 1a), it is clear that the MnO₂ nanorods exhibited a uniform diameter in the range of 100–140 nm and length of 900-1350 nm. Fig. 1b shows the wrinkled and crumpled features in FE-SEM image of GO due to sp³ carbon centres associated with oxygen functionalities and various structural defects in the basal plane of GO.¹⁷ Fig. 1c depicts the uniform distribution of MnO₂ nano-rods on the graphene oxide sheets. The EDX of GO and GOnC are shown in Fig. 2. The atomic percentage of carbon and oxygen in GO was found to be 57.91 and 42.09, respectively (Fig. 2a). However, atomic percentage of carbon, oxygen, and manganese was found to be 40.38, 43.83 and 15.79, respectively, based upon the EDX analysis of GOnC (Fig. 2b). The weight % of Mn in the GOnC, based upon EDX analysis, was found to be 38.60. The BET surface area of GOnC was found to be 156 m²g⁻¹ discerned from the nitrogen adsorption/desorption isotherm as compared with the surface area of the support graphene oxide (106 m²g⁻¹). The Raman spectrum of GO (Fig. 3a) exhibited two characteristics bands at 1598 and 1344 cm⁻¹, corresponding to G (graphitic band) and D (defects band) modes, respectively. A comparison of the Raman spectra of GO with the graphite indicated a shift in the G band towards higher wave number which is attributed to overlap of the G band with the D band due to presence of various structural defects, discrete sp² domains separated by oxygen-containing functional groups present in the GO.¹⁸ The Raman spectrum of GOnC indicated peaks corresponding

to G and D bands of GO, in addition to a sharp peak observed at 639 cm^{-1} which may be assigned to Mn–O lattice vibrations (Fig. 3b).¹⁹ The XRD pattern of GO (Fig. 4a) shows a broad diffraction peak at $2\theta = 10.89^\circ$ with a corresponding d spacing of 0.81 nm, which is very large compared to the graphite.²⁰ The ample oxygen functionalities in the basal plane of GO along with absorbed water molecules increased the interlayer distance. The XRD spectrum of GOnc (Fig 4b) depicts all peaks characteristic of MnO_2 .¹⁶ Therefore, it is concluded that the MnO_2 does not undergo any noticeable structural changes on anchoring on the GO support. The FTIR spectra of GO (Fig. 5a) exhibited strong characteristic vibrations at 3419 cm^{-1} (O–H stretch attributed to alcohol and phenol groups), 1732 cm^{-1} (C=O stretch attributed to carboxyl and carbonyl groups), 1372 cm^{-1} (O–H bending associated to phenol and alcohol groups), 1263 cm^{-1} (C–O stretch attributed to phenols, epoxy and ether groups), and 1065 cm^{-1} (C–O stretch associated to hydroxyl groups), confirming the presence of oxygen-carrying functionalities.²¹ The IR spectrum of GOnc was found to be almost identical to the IR spectrum of GO. However, an additional sharp peak observed in IR spectrum of GOnc at 597 cm^{-1} was assigned to the Mn–O stretching vibrations (Fig. 5b).²²

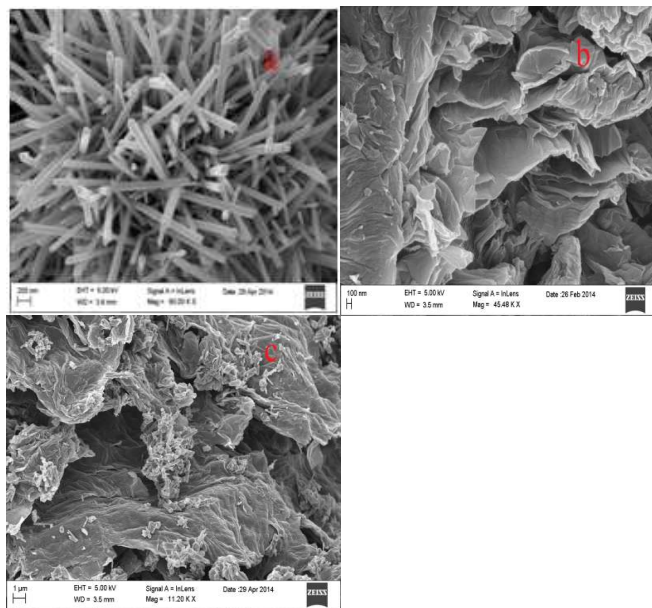


Figure 1. FE-SEM image of (a) MnO_2 nanotubes (b) GO and (c) GOnc.

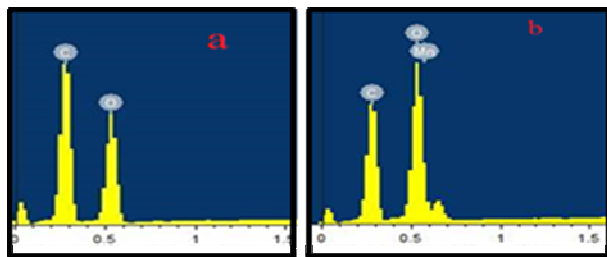


Fig. 2. EDX of (a) GO and (b) GOnc.

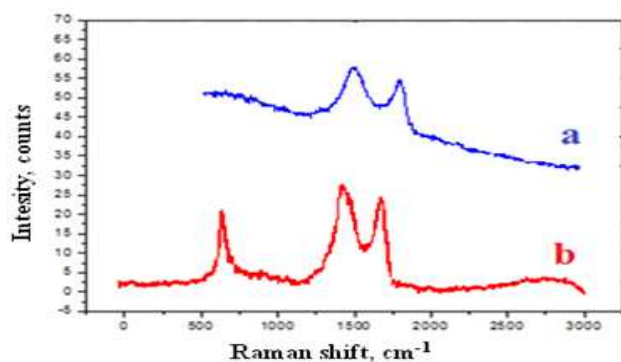


Figure 3. RAMAN spectra of GO (a) and (b) GOnc.

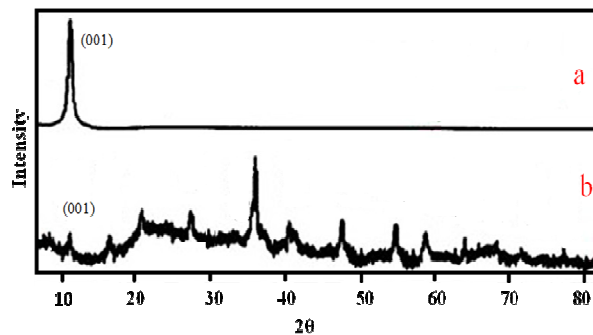


Figure 4. XRD of GO (a) and (b) GOnc.

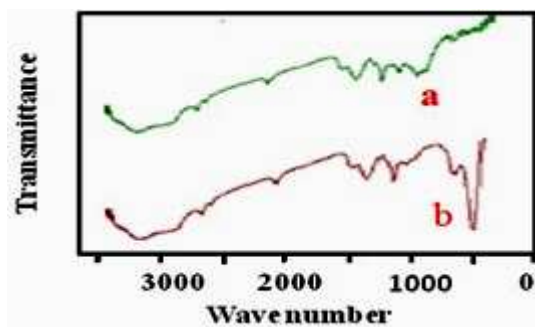
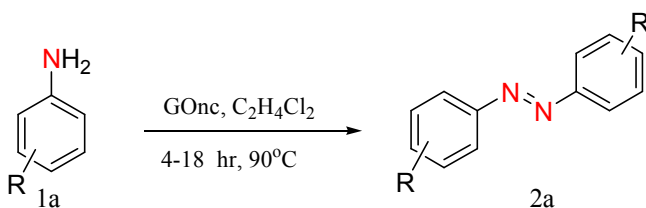


Figure 5. FTIR spectra of GO (a) and (b) GOnc.

The product of catalytic oxidation of amines mainly depends upon the nature of catalyst, as a number of products such as nitro, nitroso, azo and azoxy have been reported.¹² Therefore, in order to explore the catalytic oxidation potential and the selectivity of the synthesized GOnc composite, oxidation of a series of aromatic amines was performed under N_2 atmosphere. The catalytic performance of (5 wt %) GOnc, for the oxidation reactions of a series of aromatic amines (1 mmol) was investigated in 1,2-dichloroethane (5 mL) at reflux, for 4–7 hr to give corresponding azo- compounds (Scheme 1). Initially, aniline was chosen as a model reactant to optimize the reaction conditions. When the reaction was carried out with (5 wt %) GO as a catalyst (Table 1, entry 1), no product was obtained; only starting material was recovered as such. However, when (15 wt %) GO was used as a catalyst, poor yield of the azobenzene (< 20%) was obtained (Table 1, entry 2) with other uncharacterized by-products. MnO_2 nanorods alone (15 wt %), under identical conditions, afforded azobenzene in 50% yield. The reaction

with MnO₂ nanorods was found to be sluggish as it took almost 36 h for the completion (Table 1, entry 4) of the reaction. To our delight, the oxidation of aniline with GOnc (5 wt %) in 1,2-dichloroethane, yielded the desired product, *i.e.* azobenzene as the only product in 91% yield within 4 hr (Table 1, entry 5). This clearly indicates the better catalytic efficiency of the composite material over GO or MnO₂ nanorods alone, as a catalyst. However, no significant improvement in yield of azo-products was noticed when the catalyst loading was increased from 5 to 15 wt% under optimized reaction conditions (Table 1, entry 6).



Scheme 1 Oxidation of aromatic amines in the presence of GOnc catalyst under N₂ atmosphere to give corresponding azo compounds.

Table 1. Oxidation of aniline under different catalyst in 1,2-dichloroethane

Entry	Catalyst	Temperature, °C	Time, h	Yield, % ^a
1	5 wt % of GO	90	24	0
2	15 wt % of GO	90	48	18
3	5 wt % of MnO ₂ nanorods	90	24	45
4	15 wt % of MnO ₂ nanorods	90	36	50
5	5 wt % of GOnc	90	04	91
6	15 wt % of GOnc	90	04	92

^a Isolated yield after work up

The reaction was also carried out in different solvents such as water, ethanol, methanol, ethyl acetate, toluene, 1,2-dichloroethane and acetonitrile (Table 2). All reactions were carried out at different temperatures under reflux, corresponding to their respective boiling points. 1,2-Dichloroethane (DCE) was found to be the best solvent for the reaction. After catalyst and solvent screening, the reaction was extended to different aromatic amines bearing electron-donating and electron-withdrawing groups under similar conditions and the results obtained are summarised in Table 3. It was noted that amines bearing a electron-donating group like methoxy, methyl, in para position afforded the corresponding product with an excellent yields. However, the presence of electron-withdrawing group, retarded the oxidation of aromatic amines. Functional groups on ortho-positions had a negative influence on this reaction due to steric hindrance. These results revealed that the product yields were dependent on the substituent's position on the amines. The reaction of aliphatic amines and heteroaromatic amines like 2-aminopyridine and 2-aminobenzothiazole in place of aromatic amines under optimized reaction conditions, in presence of GOnc as a catalyst. The reaction of 2-aminopyridine yielded a complicated mixture of uncharacterized products in very low yields (< 10%) and the starting material. However, the reaction of 2-aminobenzothiazole and aliphatic amines did not succeed at all as only starting material was recovered quantitatively, thereby limiting the scope of the reaction. The products were obtained as yellow to red coloured crystalline solids, soluble in common organic solvents, and fully characterized

by IR and ¹H NMR spectra. All data matches well with the literature values.²³

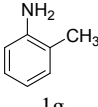
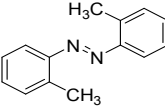
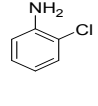
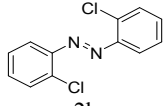
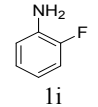
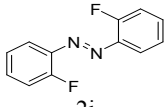
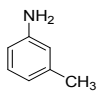
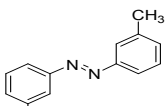
Table 2. Study of solvent effects on the reaction of aniline and GOnc as a catalyst under N₂ atmosphere at 90°C

Entry	Solvent	Time, h	Yield, % ^a
1	Water	10	33
2	Ethanol	15	45
3	Methanol	12	69
4	Acetonitrile	12	80
5	Toulene	24	55
6	1,2-Dichloroethane	04	91
7	Dichloromethane	09	75

^a Isolated yield

Table 3. Synthesis of azo compounds in presence of GOnc catalyst under N₂ atmosphere under the optimized reaction conditions

Entry	Reactant	Product ^a	Time, h	Yield, % ^b
1			4.0	91
2			6.0	85
3			7.0	89
4			8.0	79
5			7.5	81
6			9.0	71

7			8.5	75
8			13.0	69
9			18.0	50
10			10.0	75

^aPurity determined by TLC & ¹H NMR

^bIsolated yield after work up

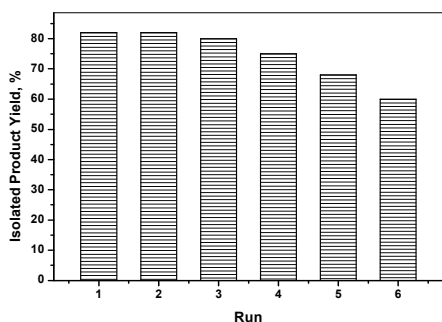


Figure 6. Recycling of GONc catalyst for the reaction of Aniline.

The recyclability of catalyst GONc was also studied by choosing aniline as model reactant. After completion of reaction catalyst can be easily filtered out from the reaction liquid phase and then washed with acetone and dried in vacuum for reuse. It is apparent from Fig.6, that the catalyst can be used three times without the significant loss of catalytic activity.

Conclusions

In summary, GONc has been synthesised and fully characterized by FE-SEM, EDX, BET surface area measurement XRD, Raman and IR spectroscopy. The GONc

has been found to be an efficient heterogeneous catalyst for the oxidation of a variety of aromatic amines to give selectively the corresponding azo-products only. The reaction provides a simple, one-step procedure for the synthesis of azo-compounds from aromatic amines in high yields.

Acknowledgements

We are thankful to the Central Instrumentation Facility of ISM for providing help in the analysis of the samples. SK acknowledges the receipt of ISM fellowship.

Notes and references

Department of Applied Chemistry, Indian School of Mines, Dhanbad-826004, India.

*Email: ddpatak@yahoo.com

Phone number: +91 9431126250.

- (a) B. F. Machado and P. Sherp, *Catal. Sci. Technol.* 2012, **2**, 54–75; (b) H. P. Jia, D. R. Dreyer and C. W. Bielawski, *Adv. Synth. Catal.*, 2011, **353**, 528–532; (c) C. Su, M. Acik, K. Takai, J. Lu, S. Hao, Y. Zheng, P. Wu, Q. Bao, T. Enoki, Y. J. Chabal and K. P. Loh, *Nat. Commun.*, 2012, **3**, 1298.
- (a) S. V. Morozov, K. S. Novoselov, M. L. Katsnelson, F. Schedin, D.C. Elias, J. A. Jaszczak and A. K. Geim, *Phys. Rev. Lett.* 2008, **100**, 16602; (b) S. Yu, Q. Liu, W. Yang, K. Han, Z. Wang and H. Zhu, *Electrochim. Acta* 2013, **94**, 245–251; (c) Y. Zhang, Y. W. Tan, H. L. Stormer and P. Kim, *Nature* 2005, **438**, 201–204.
- (a) S. S. Li, J. J. Lv, Y. Y. Hu, J. N. Zheng, J. R. Chen, A. J. Wang and J. J. Feng, *J. Power Sources* 2014, **247**, 213–218; (b) Y. L. Min, K. Zhang, W. Zhao, F. C. Zheng, Y. C. Chen and Y. G. Zhang, *Chem. Eng. J.* 2012, **194**, 203–210; (c) P. K. Khatri, S. Choudhary, R. Singh, S. L. Jain and O. P. Khatri, *Dalton Trans.* 2014, **43**, 8054–8061; (d) Y. L. Wang, P. Gao, L. H. Huang, X. J. Wu and Y. L. Liu, *Chin. J. Inorg. Chem.* 2012, **28**, 391–397; (e) Y. Q. Chen, L. B. Chen, H. Bai and L. Li, *J. Mater. Chem.* 2013, **A1**, 1992–2001.
- (a) M. Carril, R. SanMartin and E. Domínguez, *Chem. Soc. Rev.* 2008, **37**, 639–647; (b) H. J. Choi, S. M. Jung, J. M. Seo, D.W. Chang, L. Dai and J. B. Baek, *Nano Energy* 2012, **1**, 534–551; (c) G. Zhao, T. Wen, C. Chen and X. Wang, *RSC Adv.* 2012, **2**, 9286–9303; (d) Y. Gao, D. Ma, C. Wang, J. Guan and X. Bao, *Chem. Commun.* 2011, **47**, 2432–2434; (e) Y. Zhang, Z. R. Tang, X. Fu and Y. J. Xu, *Am. Chem. Soc.* 2010, **4**, 7303–7314; (f) S. Verma, H. P. Mungse, N. Kumar, S. Choudhary, S. L. Jain, B. Sain and O. P. Khatri, *Chem. Commun.*, 2011, **47**, 12673–12675.
- (a) A. V. Kumar and K. R. Rao, *Tetrahedron Lett.* 2011, **52**, 5188–5191; (b) C. Su, M. Acik, K. Takai, J. Lu, S. Hao, Y. Zheng, P. Wu, Q. Bao, T. Enoki, Y. J. Chabal and K. P. Loh, *Nature Commun.*, 2012, **3**, 1298. (c) D. R. Dreyer, H.-P. Jia and C. W. Bielawski, *Angew. Chem. Int. Ed.*, 2010, **49**, 6813–6816; (d) D. R. Dreyer, H. P. Jia, A. D. Todd, J. Geng and C. W. Bielawski, *Org. Biomol. Chem.*, 2011, **9**, 7292–7295; (e) J. Mondal, K. T. Nguyen, A. Jana, K. Kurniawan, P. Borah, Y. Zhao and A. Bhaumik, *Chem. Commun.*, 2014, **50**, 12095–12097.
- (a) L. Kesavan, R. Tiruvalam, M. H. A. Rahim, M. I. B. Saiman, D. I. Enache, R. L. Jenkins, N. Dimitratos, J. A. L. Sanchez, S. H. Taylor, D. W. Knight, C. J. Kiely and G. J. Hutchings, *Science* 2011, **331**, 195–199; (b) S. Dutta, S. Sarkar, C. Ray, A. Roy R. Sahoo, T. Pal, *ACS Applied Materials & Interfaces*, 2014, **6**, 9134–9143.
- J. Qu, L. Shi, C. He, F. Gao, B. Li, Q. Zhou, H. Hu, G. Shao, X. Wang and J. Qiu, *Carbon* 2014, **66**, 485–492.
- (a) A. Griirane, A. Corma and H. Garcia, *Nat. Protoc.* 2010, **11**, 429–438; (b) L. Fenno, O. Yizhar and K. Deisseroth, *Annu. Rev. Neurosci.* 2011, **34**, 389–412; (c) R. D. Athey Jr., *Eur. Coat. J.*, 1998, **3**, 146; (d) W. J. Sandborn, *Am. J. Gastroenterol.*, 2002, **97**, 2939–2941; (e) T. Ikeda and O. Tsutsumi, *Science*, 1995, **268**, 1873–1875.
- (a) B. L. Feringa, R. A. Van Delden, N. Koumura and E. M. Geertsema, *Chem. Rev.*, 2000, **100**, 1789–1816; (b) H. Murakami, A. Kawabuchi, K. Kotoo, M. Kutinake and N. Nakashima, *J. Am. Chem.*

- Soc.*, 1997, 119, 7605; (c) I. A. Banerjee, L. Yu and H. Matsui, *J. Am. Chem. Soc.*, 2003, **125**, 6542.
- 10 (a) E. Merino, *Chem. Soc. Rev.*, 2011, **40**, 3835–3853; (b) K. Haghbeen and E. W. Tan, *J. Org. Chem.*, 1998, **63**, 4503–4505; (c) H. H. Davey, R. D. Lee and T. J. Marks, *J. Org. Chem.*, 1999, **64**, 4976–4979; (d) E. S. Bacon and D. H. Richardson, *J. Chem. Soc.*, 1932, 884; (e) H. S. Fry, *J. Am. Chem. Soc.*, 1930, **52**, 1531; (f) J. F. Vozza, *J. Org. Chem.*, 1969, **34**, 3219; (g) T. Yamada, *Bull. Chem. Soc.*, 1969, **42**, 3565; (h) L. I. Smith and W. B. Irvine, *J. Am. Chem. Soc.*, 1941, **63**, 1036.
- 11 (a) S. Cai, H. Rong, X. Yu, X. Liu, D. Wang and W. He, *ACS Catal.* 2013, **3**, 478–486; (b) A. Grirrane, A. Corma and H. Garcia, *Science* 2008, **322**, 1661–1664; (c) Y. Zhu and Y. Shi, *Org. Lett.* 2013, **15**, 1942–1945; (d) L. Hu, X. Cao, L. Chen, J. Zheng, J. Lu, X. Sun and H. Gu, *Chem. Commun.* 2012, **48**, 3445–3447; (e) M. Fetizon, M. Golfier, R. Milcent and I. Papadakis, *Tetrahedron* 1975, **31**, 165–170; (f) H. K. Hombrecher and K. Lu^{dtke}, *Tetrahedron*, 1993, **49**, 9489–9494; (g) H. Firouzabadi, B. Vessal and M. Naderi, *Tetrahedron Lett.* 1982, **23**, 1847–1850; (h) G. Crank and M. I. H. Makin, *Aust. J. Chem.*, 1984, **37**, 845–855; (i) E. Baer and A. L. Tosoni, *J. Am. Chem. Soc.*, 1956, **78**, 2857–2858; (j) S. Okumura, C. H. Lin, Y. Takeda, and S. Minakata, *J. Org. Chem.* 2013, **78**, 12090–12105; (k) Y. Takeda, S. Okumura, and S. Minakata, *Angew. Chem. Int. Ed.* 2012, **51**, 7804–7808 (l) K. Nakagawa and T. Tsuji, *Chem. Pharm. Bull.*, 1963, **11**, 296–301; (m) H. Firouzabadi and Z. Mostafavipoor, *Synth. Commun.*, 1984, **14**, 875–882; (n) H. Firouzabadi and Z. Mostafavipoor, *Bull. Chem. Soc. Jpn.*, 1983, **56**, 914.
- 12 L. Lekha, K. K. Raja, G. Rajagopal and D. Easwaramoorthy, *J. Organomet. Chem.* 2014, **753**, 72–80.
- 13 W. Lu and C. Xi, *Tetrahedron Lett.* 2008, **49**, 4011–4015.
- 14 N. Tang, X. Tian, C. Yang, Z. Pi and Q. Han, *J. Phys. Chem. Solids* 2010, **71**, 258–262.
- 15 N.I. Kovtyukhova, P.J. Ollivier, B.R. Martin, T.E. Mallouk, S.A. Chizhik, E.V. Buzaneva and A.D. Gorchinskiy, *Chem. Mater.* 1999, **11**, 771–778.
- 16 G. G. Kumar, Z. Awan, K. S. Nahm and J. S. Xavier, *Biosens. Bioelectron.* 2014, **53**, 528–534.
- 17 S. Kumari, A. Shekhar, H. P. Mungse, O. P. Khatri, D. D. Pathak, *RSC Adv.*, 2014, **4**, 41690–41695.
- 18 (a) G. K. Ramesha and S. Sampath, *J. Phys. Chem. Lett.*, 2009, 113, 7985; (b) K. N. Kudin, B. Ozbas, H. C. Schniepp, R. K. Prud'homme, I. A. Aksay and R. Car, *Nano Lett.*, 2008, **8**, 36; (c) Z. H. Ni, Y. Y. Wang, T. Yu and Z. X. Shen, *Nano Research* 2008, **1**, 273–291.
- 19 M. Kim, Y. Hwang and J. Kim, *J. Power Sources* 2013, **239**, 225–233.
- 20 A.C. Ferrari, *Solid State Communications*, 2007, **143** 47–57.
- 21 (a) A. Bagri, C. Mattevi, M. Acik, Y. J. Chabal, M. Chhowalla and V. B. Shenoy, *Nat. Chem.*, 2010, **2**, 581–587; (b) H. P. Mungse, O. P. Sharma, H. Sugimura and O. P. Khatri, *RSC Adv.*, 2014, **4**, 22589–22595.
- 22 S. Chen, J. Zhu, X. Wu, Q. Han and X. Wang, *ACS Nano* 2010, **4**, 2822–2830.
- 23 N. Sakai, S. Asama, S. Anai, and T. Konakahara, *Tetrahedron*, 2014, **70**, 2027–2033.

Graphical Abstract

